

# XAFS Study of Some Titanium Silicon and Germanium Compounds

To cite this article: D. B. Aldrich *et al* 1993 *Jpn. J. Appl. Phys.* **32** 725

View the [article online](#) for updates and enhancements.

## You may also like

- [Enhancement Effect of C40 TiSi<sub>2</sub> on the C54 Phase Formation](#)  
S. Y. Chen, Z. X. Shen, A. K. See *et al.*
- [Gold Superfill in Sub-Micrometer Trenches](#)  
D. Josell, C. R. Beauchamp, D. R. Kelley *et al.*
- [Deposition Behavior of Ni on Si\(100\) Surfaces in an Aqueous Alkaline Solution](#)  
Daisuke Niwa, Takayuki Homma and Tetsuya Osaka

## Recent citations

- [Silicide formation and stability of](#)  
Zhihai Wang *et al*
- [A low-temperature total electron yield detector for x-ray absorption fine structure spectra](#)  
K. M. Kemner *et al*

## XAFS Study of Some Titanium Silicon and Germanium Compounds

D.B. ALDRICH, R.J. NEMANICH, and D.E. SAYERS

Department of Physics, North Carolina State University, Raleigh, North Carolina, USA 27595-8202

(Received August 24, 1992)

It has been shown that, across the full range of Si-Ge alloy compositions,  $C54 Ti(Si_yGe_{1-y})_2$  will form from the reaction of Ti with  $Si_xGe_{1-x}$ . An increase in the silicon fraction (i.e.,  $y > x$ ) was seen with the formation of Titanium Germanosilicide which may be due, in part, to the relative diffusion rates of Si and Ge in Ti. In  $C54 Ti(Si_yGe_{1-y})_2$  the Si and Ge atoms occupy sites equivalent to the Si in  $C54 TiSi_2$ . Within error, these atoms form shells about the Ti atoms, with Si and Ge occupancies indicative of the net Si and Ge atomic percents. The radial distances of the shells vary linearly, within error, between those of  $C54 TiSi_2$  and  $C54 TiGe_2$ . The ability to vary the shell distances (and thus vary the lattice constants) of  $C54 Ti(Si_yGe_{1-y})_2$  by varying Si and Ge content will prove useful in applications where lattice matching and epitaxy are of importance.

**KEYWORDS:** EXAFS, C54, Ti, Si, Ge,  $Ti(Si_yGe_{1-y})_2$ , alloy, titanium germanosilicide, metallization

### §1. INTRODUCTION

Titanium silicide is of interest for use in contacts and interconnects in VLSI applications because of its low resistivity. Metallized Ge and Si-Ge alloys are being investigated for similar use in advanced silicon based device structures. Integration of such materials will require a thorough understanding of the reactions involved. The Ti-Si and Ti-Ge reactions have been the subject of previous studies<sup>1,2)</sup>. Reaction of a thin titanium film with pure silicon produces either C49  $TiSi_2$  or C54  $TiSi_2$ , depending on the energetics of the system. The metastable C49 phase usually forms at intermediate temperatures (after some short range intermixing at low temperatures) as a precursor to the C54 phase which forms at high temperatures. The C54 phase is thought to have a lower bulk free energy making it the stable  $TiSi_2$  phase. A thin titanium film will react with pure germanium in two stages; but, unlike the Ti-Si reaction, there is a stoichiometric change between phases. At intermediate temperatures  $Ti_6Ge_5$  forms, followed, at high temperatures, by C54  $TiGe_2$ . The C54  $TiGe_2$  is isomorphic with C54  $TiSi_2$ . Silicon and germanium atoms occupy equivalent positions in C54  $TiSi_2$  and C54  $TiGe_2$  respectively, and it has been proposed that the high temperature reaction of Ti with  $Si_xGe_{1-x}$  alloy will result in the formation of  $C54 Ti(Si_xGe_{1-x})_2$  which is isomorphic with C54  $TiSi_2$ <sup>3)</sup>. There is no equivalent in the Ti-Si system to  $Ti_6Ge_5$ , nor has a C49 structure of  $TiGe_2$  been observed. The different reaction paths of Ti-Si and Ti-Ge may affect the  $Ti-Si_xGe_{1-x}$  reaction path, causing Ti-Si / Ti-Ge segregation during the initial stages of the reaction. This work focuses on changes in the composition and microstructure of reacted Ti-Si-Ge with respect to changes in pre-reaction Si-Ge alloy composition. Auger Electron Spectroscopy (AES) was used to examine composition, and X-Ray Absorption Fine Structure (XAFS) was used to examine microstructure.

### §2. EXPERIMENTAL

Samples were prepared by UHV deposition of Si,  $Si_xGe_{1-x}$  and Ti layers on Si(100) wafers and then *in situ* annealing. The deposition system has a heated sample stage for *in situ* annealing, titanium deposition filaments,

two electron beam evaporation sources for Si-Ge alloy deposition and a base pressure of  $< 8 \times 10^{-11}$  torr. The wafer cleaning process used is outlined elsewhere<sup>4)</sup> and is known to produce atomically clean surfaces. Substrate temperature was held at 550°C for deposition of a homoepitaxial silicon base layer (300Å-400Å) and a Si-Ge alloy layer (2000Å-2500Å). Substrate temperature was decreased to below 150°C prior to deposition of a 400Å titanium layer. The samples subsequently were annealed at 700°C, 750°C, or 850°C for 10 minutes or 750°C for 100 minutes *in situ*.

Depth profile composition measurements were performed in a Japan Electron Optics Ltd. (JEOL) JAMP-30 Auger system. The Auger microprobe was positioned using Secondary Electron Microscopy (SEM). Auger data collection and sample sputtering were cycled until the composition of the region of interest was determined. The carbon and oxygen Auger signals were recorded, along with Ti, Si and Ge Auger signals, to check for the presence of these contaminants. Standard Si-Ge alloy samples (previously analyzed by RBS) were used to check relative Si and Ge Auger sensitivities.

The XAFS measurements were taken at beam line X-11A of the National Synchrotron Light Source (NSLS) at Brookhaven National Laboratory (BNL). All measurements were carried out at the titanium K edge (4966 eV). Electron beam energy was either 2.53 GeV or 2.58 GeV with a stored current between 100 mA and 220 mA. The X-ray energy was defined by a double crystal monochromator with Si(111) crystals. The crystals were detuned 50%-60% at 5366 eV for harmonic rejection. The energy calibration was periodically checked using a titanium foil in transmission. An electron yield detector with both sample tilt and rotation capabilities was used in a low angle configuration to minimize Bragg reflections. The specific detector design has been described elsewhere<sup>5)</sup>. Helium was used in the detector and in the beam path, when possible, to increase efficiency. Data was collected at room temperature and edge steps of 0.2 to 3.5 were typical. Increased integration time in the 381 eV - 975 eV region (above the absorption edge) was used to improve the signal/noise ratio. Data analysis was performed using the Eindhoven background subtraction, Fourier filtering and fitting programs. Typical Fourier filtering parameters were: K weight = 2, K range =  $2-12 \text{ \AA}^{-1}$  and R range = 1.5 - 3.5 ( $\Delta R \Delta K / \pi = 6.37$ ). During fitting, a maximum of six

parameters very varied per iteration. Theoretical phase shift files generated by FEFF3 were used in the fitting.

§3. RESULTS

To examine the effect of deposited  $\text{Si}_x\text{Ge}_{1-x}$  composition on the composition and microstructure of the reacted  $\text{Ti-Si}_x\text{Ge}_{1-x}$ , a series of samples annealed at  $750^\circ\text{C}$  for 10 minutes was produced. Deposited  $\text{Si}_x\text{Ge}_{1-x}$  compositions of  $x = 0.69, 0.63, 0.45, 0.40, 0.30$ , and  $0.21$  were used. Auger compositional analysis indicated that the reacted material was  $\text{Ti}(\text{Si}_y\text{Ge}_{1-y})_2$ . Auger microprobe compositional analysis also revealed Si-Ge segregation. Composition of the  $\text{Ti}(\text{Si}_y\text{Ge}_{1-y})_2$  was silicon rich compared to the original  $\text{Si}_x\text{Ge}_{1-x}$  alloy (i.e.,  $y > x$ ). The  $\text{Si}_z\text{Ge}_{1-z}$  immediately surrounding the  $\text{Ti}(\text{Si}_y\text{Ge}_{1-y})_2$  was found to be Si poor (i.e.,  $y > x > z$ ). Deviations from the original Si-Ge alloy composition were greatest for the  $x=0.45$  sample.

The  $k^2$  weighted EXAFS chi data of the  $750^\circ\text{C}/10$  min. samples appears in Fig. 1. Characteristics of C54  $\text{TiSi}_2$  can be seen in the  $x=0.69$  and  $x=0.63$  samples and characteristics of C54  $\text{TiGe}_2$  can be seen in the  $x=0.30$  and  $x=0.21$  samples. The samples from the intermediate region ( $x=0.45$  and  $0.40$ ) contain features of both materials. The Fourier transformed chi data, (Figure 2) shows a continuous transition between  $\text{TiSi}_2$  and  $\text{TiGe}_2$ .

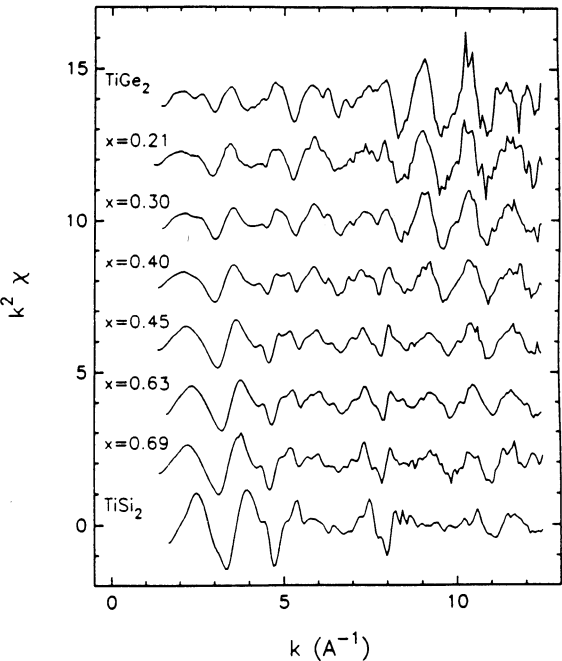


Fig. 1.  $k^2$  weighted EXAFS of  $\text{Ti}(\text{Si}_y\text{Ge}_{1-y})_2$  (indexed by Si fraction of deposited  $\text{Si}_x\text{Ge}_{1-x}$ ).

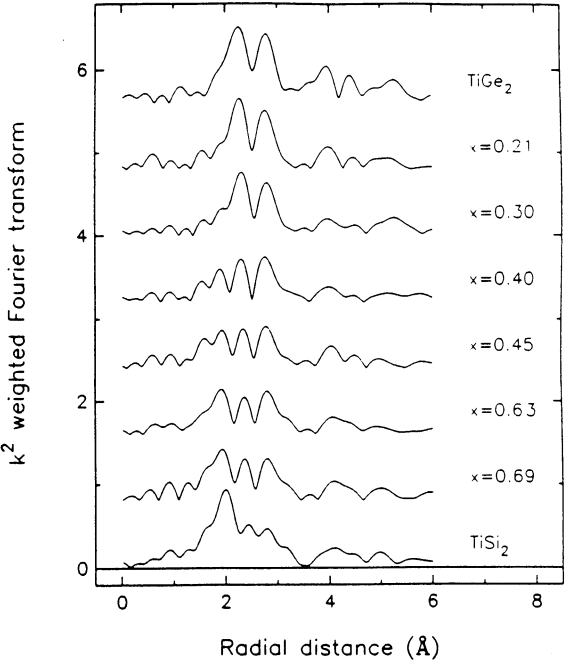


FIG. 2. Fourier transform of  $\text{Ti}(\text{Si}_y\text{Ge}_{1-y})_2$  EXAFS (indexed by Si fraction of deposited  $\text{Si}_x\text{Ge}_{1-x}$ ).

In both crystalline titanium disilicide and digermanide the Ti atoms have four inseparable near-neighbor shells: Viz. 4 Si -  $2.553\text{\AA}$ , 4 Si -  $2.745\text{\AA}$ , 2 Si -  $2.781\text{\AA}$ , 4 Ti -  $3.206\text{\AA}$ , and 4 Ge -  $2.596\text{\AA}$ , 4 Ge -  $2.916\text{\AA}$ , 2 Ge -  $2.954\text{\AA}$ , 4 Ti -  $3.332\text{\AA}$  respectively<sup>6</sup>). The best fits of the EXAFS of C54  $\text{TiSi}_2$  and C54  $\text{TiGe}_2$  standard samples were used as a starting point for fitting the EXAFS of the  $750^\circ\text{C}/10$  min. samples. Five shells were used in fitting the  $\text{Ti}(\text{Si}_y\text{Ge}_{1-y})_2$  (Ti-Si, Ti-Ge, Ti-Si, Ti-Ge, Ti-Ti). The C54  $\text{TiSi}_2$  Ti-Ti shell and the C54  $\text{TiGe}_2$  Ti-Ti shell routinely converged and they were replaced with one Ti-Ti shell.

The five shell fitting results (see Table I) indicate that, in a given sample, the first Ti-Si shell distance and first Ti-Ge shell distance converge to form a single shell with mixed Si and Ge occupancy (likewise for the second Ti-Si shell and second Ti-Ge shell). Plotting and linear fitting of the shell distances (see Figure 3) indicate that there is a linear dependence of shell distances upon the silicon atomic fraction. Ratios of the Si and Ge occupancies are in good agreement with the Si and Ge content indicated by Auger analysis.

Table I. Fitted parameters of  $\text{Ti}(\text{Si}_y\text{Ge}_{1-y})_2$  (indexed by shell and by Si fraction of deposited  $\text{Si}_x\text{Ge}_{1-x}$ ).

X	N	R (Å)	$\sigma^2 (10^{-4}\text{\AA}^2)$	$\Delta E0$
FIRST Ti-Si SHELL				
1.00	2.96	2.54	35	-1.04
0.69	2.24	2.57	45	3.06
0.63	2.32	2.59	39	0.13
0.45	1.90	2.69	33	0.22
0.40	1.23	2.60	21	3.38
0.30	1.07	2.62	42	2.79
0.21	0.94	2.62	46	6.00

## FIRST Ti-Ge SHELL

0.69	0.58	2.57	59	3.77
0.63	1.21	2.57	39	1.05
0.45	1.05	2.57	35	0.73
0.40	1.53	2.59	24	2.81
0.30	2.10	2.59	29	2.93
0.21	2.35	2.59	30	5.17
0.00	3.44	2.61	37	-1.17

## SECOND Ti-Si SHELL

1.00	5.30	2.74	88	0.45
0.69	3.45	2.79	73	2.30
0.63	2.85	2.80	90	1.39
0.45	3.31	2.81	83	1.13
0.40	2.07	2.84	76	2.04
0.30	1.12	2.85	100	1.69
0.21	0.81	2.87	93	1.95

## SECOND Ti-Ge SHELL

0.69	0.88	2.81	106	2.98
0.63	1.73	2.80	105	3.61
0.45	1.89	2.80	95	1.94
0.40	2.64	2.81	82	2.31
0.30	2.05	2.84	99	2.18
0.21	2.36	2.84	91	3.03
0.00	5.22	2.84	95	0.53

## Ti-Ti SHELL

1.00	1.71	3.21	32	-1.20
0.69	1.93	3.25	23	2.27
0.63	1.88	3.22	29	2.21
0.45	1.73	3.23	32	4.12
0.40	1.32	3.27	25	3.80
0.30	1.55	3.29	15	4.12
0.21	1.90	3.29	24	6.55
0.00	1.60	3.32	38	2.58

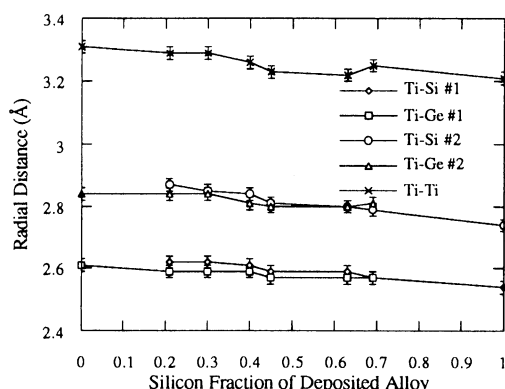


FIG. 3. Variation of  $\text{Ti}(\text{Si}_y\text{Ge}_{1-y})_2$  shell distances with deposited alloy composition.

#### §4. CONCLUSION

Titanium has been shown to react with Si-Ge alloys to form a  $\text{Ti}(\text{Si}_y\text{Ge}_{1-y})_2$  compound with C54 structure. The Si/Ge ratio in the reacted  $\text{Ti}(\text{Si}_y\text{Ge}_{1-y})_2$  is greater than in the deposited  $\text{Si}_x\text{Ge}_{1-x}$ . This may be caused by the diffusion properties of silicon, titanium, and germanium or by the competing Ti-Si and Ti-Ge reaction paths. In the Ti-Si reaction, silicon is the dominant diffusing species<sup>7)</sup>. In the Ti-Ge reaction, titanium is thought to be the dominant diffusing species. If these relationships hold, the Ti-Si-Ge reaction then Si and Ti will interdiffuse and react more rapidly than Ge and Ti.

In Si-Ge alloy the Si-Si and Ge-Ge bond lengths vary with alloy composition. On a macroscopic scale the Si-Ge alloy crystal has an effective lattice constant which is a weighted average of the silicon and germanium lattice

constants. On the microscopic scale there are still distinctly different bond lengths for Si-Si, Si-Ge, and Ge-Ge bonds.  $\text{Ti}(\text{Si}_y\text{Ge}_{1-y})_2$  does not exhibit this type of behavior. Attempts were made to fit the  $\text{Ti}(\text{Si}_y\text{Ge}_{1-y})_2$  samples with distinctly different shell distances for Ti-Si and Ti-Ge shells. In all cases, the fits progressed toward shells with both Si and Ge occupancy.

There is good agreement between Si/Ge shell occupancy ratios calculated from the EXAFS fitting results and Si/Ge atomic fraction ratios calculated from the Auger compositional analysis. This is because in the C54  $\text{Ti}(\text{Si}_y\text{Ge}_{1-y})_2$  structure all of the Si/Ge sites are equivalent (each Si/Ge site is a nearest neighbor to two Ti atoms and next-nearest neighbor to three Ti atoms)<sup>6)</sup>. Rearrangement of the Si and Ge atoms on the lattice will not affect the average Ti-Si/Ge shell occupancies. To investigate Si-Ge segregation in  $\text{Ti}(\text{Si}_y\text{Ge}_{1-y})_2$  it will be necessary to examine the microstructure of the Ge or Si atoms by analyzing the Ge or Si EXAFS respectively.

#### ACKNOWLEDGMENTS

The authors would like to thank the following persons for their assistance in data collection and analysis and for insightful scientific discussions: S. Ashburn, Y. Dao, A.M. Edwards, M. Joo, K. Kemner, and C. Sukow. This work was supported in part by the Division of Materials Science of the Department of Energy under contract DE-FG05-89ER45384 and by the National Science Foundation through grant DMR 8717816.

#### REFERENCES

- 1) D.B. Aldrich, Q. Islam, H. Jeon, R.J. Nemanich, and D.E. Sayers, *Mat. Res. Soc. Symp. Proc.*, **159** (1990) 167.
- 2) D.B. Aldrich, C. L. Jahncke, R. J. Nemanich, and D. E. Sayers, *Mat. Res. Soc. Symp. Proc.*, **221** (1991) 343.
- 3) O. Thomas, F.M. d'Heurle, and S. Delage, *J. Mater. Res.* **5** (1990) 1453.
- 4) H. Jeon, C.A. Sukow, J.W. Honeycutt, T.P. Humphreys, R.J. Nemanich, and G.A. Rozgonyi, *Mat. Res. Soc. Symp. Proc.*, **181** (1991) 559.
- 5) K. Kemner, Z. Wang, R.A. Mayanovic, B.A. Bunker, *Nuclear Instr. and Meth.* (to be published)
- 6) P. Villars and L.D. Calvert, *Pearson's Handbook of Crystallographic Data for Intermetallic Phases* (American Society for Metals, Metals Park, OH, 1986), pp.2435, 3194.
- 7) A.P. Botha and R. Pretorius, *Thin Solid Films*, **93** (1982) 127.